ORIGINAL RESEARCH

Production and Characterization of Type III Resistant Starch from Native Wheat Starch Using Thermal and Enzymatic Modifications

Carlos Gabriel Arp[1] · María Jimena Correa[1] · Cristina Ferrero[1]

Abstract

The most widely employed methodologies for type III (retrograded) resistant starch formation is a cyclic heating-cooling treatment or its combination with a previous enzymatic debranching step. In this work, two retrogradation temperatures, 0 and 4 °C, were evaluated for obtaining type III resistant starch from non-debranched and pullulanase-debranched wheat starch. The starches were characterized by their thermal and pasting behavior. Also, microstructural and crystalline aspects were related to the production process and the nutritional properties of the products. The most influencing factor for resistant starch formation was the application of the pullulanase-debranching step previous to the cyclic treatment. This led to a higher starch retrogradation and a more compact microstructure, which decreased the thickening capacity and the digestibility of the starches. Then, even though all the obtained starches exhibited lower digestibility, the pullulanase-debranched ones presented the lowest estimated glycemic index (ca. 34%), showing the highest yield of resistant starch formation. Finally, this work presents a concise protocol for obtaining type III resistant starch enriched powder with low digestibility that could be used in the formulation of different healthy foods such as dairy products, cereal bars, and even drinks.

Keywords Resistant wheat starch · Pullulanase · DSC · X-ray diffraction · Starch digestibility

Introduction

Resistant starches are functional ingredients with multiple health benefits when they are consumed in a regular diet. The formulation of food products with resistant starch (RS) gives low-calorie and low-glycemic index meals, with less available carbohydrate content and rich in dietary fiber (Wong and Louie 2017). Moreover, it has been established that these functional ingredients exert a prebiotic effect.

Resistant starch can be fermented by beneficial colorectal *Lactobacilli* and *Bifidobacteria*, favoring their growth and producing short-chain fatty acids (SCFAs) (Gopalsamy et al. 2019; Li et al. 2018).

These healthy starches are classified into different types depending on the characteristics that confer their resistance to enzymatic hydrolysis. Thus, type I resistant starches (RSI) are native starches physically protected from hydrolysis by vegetable material, such as plant cell walls. Type II resistant starches (RSII) are native starches, mainly consisting of high-amylose starch, with a compact crystalline granular structure that prevents α-amylase digestion. Type III resistant starches (RSIII) are formed by recrystallization of the starch polymers (amylose and amylopectin) during cooling and aging of gelatinized starch in a process called retrogradation. In these cases, it has been established that the enzyme action is avoided by the new crystalline arrangement. Other resistant starch types are RSIV (chemically modified starch) and RSV (amylose–lipid complex) (Jiang et al. 2020).

Due not only to its nutritional benefits but also to its technological advantages that ease its incorporation into

✉ Carlos Gabriel Arp
carp@exactas.unlp.edu.ar

María Jimena Correa
mjcorrea@biol.unlp.edu.ar

Cristina Ferrero
cferrero@biol.unlp.edu.ar

[1] Centro de Investigación y Desarrollo en Criotecnología de Alimentos (CIDCA), Comisión de Investigaciones Científicas de la Provincia de Buenos Aires, Consejo Nacional de Investigaciones Científicas y Técnicas, Facultad de Ciencias Exactas, Universidad Nacional de La Plata, 47 y 116, 1900 La Plata, Argentina

different foods (e.g., low particle size, white color and bland flavor), many efforts have been made to produce resistant starch, several of them dedicated to the type III. For this purpose, native starches from very different botanical origins, i.e., starches from legumes (Chávez-Murillo et al. 2018; Dong and Vasanthan 2020; Remya et al. 2018) and grains (Khan et al. 2019; Van Hung et al. 2020), with particular focus on high-amylose corn starch (Dundar and Gocmen 2013; Öztürk and Köksel 2014), waxy maize starch (Chang et al. 2020; Shi et al. 2018), and normal maize starch (Liu et al. 2014; Zhang and Jin 2011), were modified by several methods. Moreover, other starch sources such as roots and tubers (Remya et al. 2018; Wandee et al. 2012; Zhao et al. 2018), unripe banana (Cordoba et al. 2018; Remya et al. 2018), and sago palm (Pratiwi et al. 2015), among others, were also used for this purpose. Some of these type III resistant starches are commercially available (such as Novelose®330, C*Actistar and Neo-amylose) and have been applied in several foods aiming to obtain healthier products. Due to their stability to heating processes, these ingredients can be often found not only in extruded products and batter-fried foods but also in beverages (Bello-Perez and Hoyos-Leyva 2018; Champ 2004).

Several authors proposed that the application of thermal enzymatic treatments over starch samples, in combination or not with previous enzymatic hydrolysis, would increase their type III resistant starch content, reducing or slowing the digestibility and then lowering the glycemic index (Ashwar et al. 2016; Pratiwi et al. 2018). Nonetheless, even though wheat is the cereal product more widely employed as raw material for the production of baked goods and pastry around the world, in the past decades, only few works have focused on the formation and quantification of type III resistant starches in wheat products (Brumovsky et al. 2009; Yadav et al. 2010). However, this starch source could yield a good level of resistant starch if a suitable process is applied. Given the need for more thorough knowledge, this work aims to study the processes related to wheat starch retrogradation not only focusing especially on type III resistant starch formation but also analyzing its thermal and pasting behavior, as well as its microstructural and nutritional aspects.

Materials and Methods

Materials

Native wheat starch (NS) was purchased from Bernesa S.A.C.I (Argentina), and pullulanase enzyme (EC 3.2.1.41) was acquired from Sigma-Aldrich (Argentina). All enzymes and reagents were of analytical grade.

Resistant Starch Formation

Starches were modified by thermal treatment and enzymatic-thermal treatment. First, NS suspensions (10% w/w in distilled water) were gelatinized in a water bath at 85 °C for 30 min under stirring. Then, samples were cooled and incubated in a shaking water bath at 59 °C for 6 h without or with pullulanase (20 ASPU/g NS). After incubation, the samples were subjected to a cyclic thermal treatment consisting of heating the suspensions at 121 °C for 30 min in an autoclave, followed by a 24 h period of storage in a chamber at 0 or 4 °C for retrogradation. The cyclic heating-cooling treatment was repeated four times. Then, the obtained product was freeze-dried and ground to powder. The samples obtained by this procedure were identified as RSp0 and RSp4 depending on their corresponding storage temperatures (Fig. 1). Also, retrograded starch powders prepared only by thermal treatment were identified as RS0 and RS4, depending on whether the storage temperature was 0 °C or 4 °C, respectively (Fig. 1).
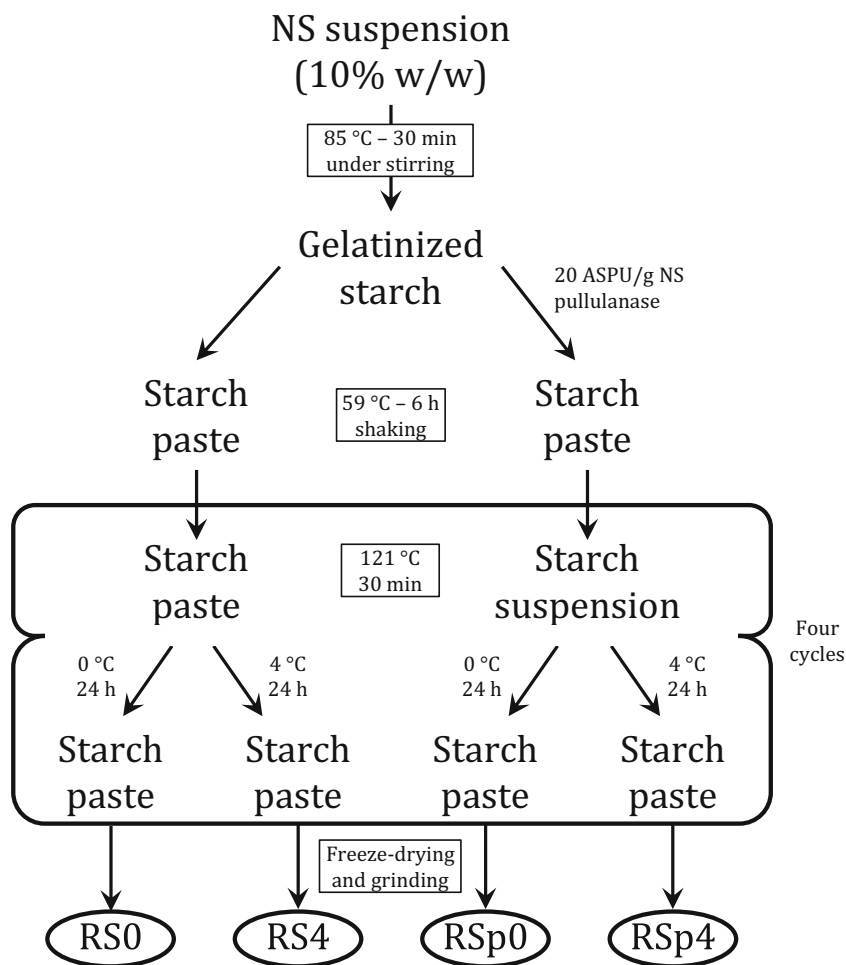
Thermal Properties by DSC

Starch powders were subjected to heating in a Q100 differential scanning calorimeter (TA Instruments, USA) for the evaluation of thermal transitions in the range from 5 to 140 °C. DSC runs were performed with a 10 °C/min heating rate. DSC pans containing approximately 10 mg of starch suspension (1:3 in distilled water) were hermetically sealed and left to rest for 3 h at room temperature previous to the assay. A 5-min isotherm at 5 °C was employed for thermal stabilization. The following thermal parameters were evaluated for each transition found: melting enthalpy (ΔH), onset, peak, and final temperatures (T_o, T_p, T_f, respectively) and transition temperature range (ΔT). The additional subscripts R and A-L will indicate if the parameter corresponds to the retrograded amylopectin melting or the amylose–lipid complex dissociation, respectively. The assays were done at least in triplicate.

Pasting Properties

The pasting properties of NS and retrograded starches were evaluated in an RVA 4500 (Perten Instruments, Australia) according to the AACC 76-21.01 approved method (AACC International 2009). Starch (3.00 g) and water (25.0 g) were weighed in an aluminum container and rapidly mixed by vertically shaking the stirrer ten times. Then, the suspension was immediately placed in the measuring position and the program started. The following parameters were determined using the specialized software Thermocline for Windows (TCW) version 3.16.1.387 (Perten Instruments, Australia) provided with the instrument: pasting temperature (T_e), pasting time (t_e), peak viscosity (η_p), minimum viscosity or through (η_{min}), breakdown or difference between peak and minimum

Fig. 1 Preparation of type III resistant starch from native wheat starch

NS suspension
(10% w/w)

85 °C – 30 min under stirring

Gelatinized starch

20 ASPU/g NS pullulanase

Starch paste

59 °C – 6 h shaking

Starch paste

Starch paste

121 °C 30 min

Starch suspension

Four cycles

0 °C 24 h

4 °C 24 h

0 °C 24 h

4 °C 24 h

Starch paste

Starch paste

Starch paste

Starch paste

Freeze-drying and grinding

RS0

RS4

RSp0

RSp4

viscosity (η_p–η_{min}), final viscosity (η_f), setback 1 or the difference between final and minimum viscosity (η_f–η_{min}), and setback 2 or the difference between final and peak viscosity (η_f–η_p).

LVSEM

Starch powders were observed in a FEI Quanta 200 low-vacuum scanning electron microscopy (LVSEM) at 130 Pa using a secondary electron detector. First, the powders were mounted on an aluminum base using double-sided stick tape and then placed in the observation chamber of the microscope. Images were taken at 400× at "Servicio de Microscopía Electrónica y Microanálisis (SeMFi-LIMF)—Facultad de Ingeniería, UNLP, Argentina."

X-ray Diffraction

X-ray diffraction patterns of NS and resistant starch powders were acquired at 40 V and 40 mA with Cu-Kα radiation in an X'Pert PRO X-ray diffractometer (PANalytical, the Netherlands). The samples were scanned at a scanning rate

of 1°/min in a 4–40° Bragg's angle range. The analysis of the diffraction patterns was performed with PeakFit v4.12 (SeaSolve Software Inc., USA).

In Vitro Starch Digestibility and Estimated GI

Hydrolysis of the obtained RS powders was carried out with α-amylase following the method described by Arp et al. (2018). First, approximately 500 mg of each starch was exactly weighed and suspended in 25 mL phosphate buffer (pH 6.9) in 50-mL conical plastic tubes. Tubes were then placed in a heat block at 37 °C with shaking (650 rpm). Afterward, 5 mL α-amylase solution (10.31 U/mL, containing 20 μL CaCl$_2$ 3 M) was added to each tube while keeping incubation temperature and shaking. Hereafter, 200-μL aliquots were taken at time 0 (right after enzyme addition), 20, 60, 90, and 120 min and were placed in tubes in a boiling water bath (5 min) for enzyme deactivation. Quantification of released reducing sugars in the aliquots was carried out by 3,5-dinitrosalicylic acid (DNS) method at 530 nm. The data was used to build hydrolysis curves. Then, all curves were fitted to a model equation proposed by Goñi et al. (1997) (Eq. 1).

$$C = C_\infty \left(1 - e^{-kt}\right) \qquad (1)$$

where C is the reducing sugars released by hydrolysis at a given time, t; C_∞ is the limit digestibility (value of C at $t \to \infty$); and k is the constant rate.

For comparison purposes, hydrolysis analysis of NS was also performed. In the case of native or uncooked starches, gelatinization must be achieved prior to the assays (Goñi et al. 1997). So, the NS was gelatinized by heating for 30 min in boiling phosphate buffer. Then, the suspension was treated as described in the above paragraph.

Finally, the glycemic index (GI) was estimated as proposed by Goñi et al. (1997). The procedure involves integrating each curve for obtaining the respective area under the curve and then calculating the estimated GI as the mathematical ratio of the area of each retrograded starch with the one corresponding to the NS (taken as 100%).

Statistical Analysis

Means were compared by two-way analysis of variance (ANOVA) and LSD Fisher test at a 0.05 significance level using the statistical analysis software InfoStat 2018e. The factors were "pullulanase treatment" and "retrogradation temperature." On the other hand, the curve fittings and dataset comparisons with F test at 95% confidence level were performed with OriginPro 8.

Results and Discussion

Thermal Analysis

The thermal parameters of the rehydrated starch powders are shown in Table 1. All samples exhibited two endotherms.

Those occurring in the temperature range from 36 to 86 °C were associated with retrograded amylopectin melting, while those that took place over 88 °C were related to the amylose–lipid complex dissociation (Kovrlija and Rondeau-Mouro 2017; Yu et al. 2018).

With respect to the retrograded amylopectin melting, RS0 and RS4 showed small endotherms with lower transition enthalpies in a relatively narrower temperature range. On the contrary, the pullulanase-treated samples presented wider endotherms with markedly higher enthalpies, suggesting that the amylopectin debranching step favored the retrogradation. Moreover, for the mentioned parameters, significant interactions were found between the two evaluated factors: "pullulanase treatment" and "retrogradation temperature", and a tendency to higher ΔH_R was found when enzymatically treated samples were stored at 4 °C ($p = 0.0511$). Given that pullulanase is an enzyme that hydrolyses α ($1 \to 6$) glycosidic bonds, its action on amylopectin releases chains with different polymerization and branching degrees. The higher number of free longer chains (those left behind by releasing the branches) would enhance the effectiveness for chain–chain interactions, favoring the re-association of the amylopectin molecules and thus explaining the increase in the enthalpy of the pullulanase-treated samples. On the other hand, the length heterogeneity of the released chains is reflected in the temperature range (ΔT_R) of the melting transition (Table 1).

Two consecutive events occur in retrograding starchy systems that favor the recrystallization process. Firstly, nucleation implies aggregation of polysaccharide chains, a process that is favored by low temperature, and then follows propagation or crystal growth, where double helices are formed and assembled. This step is favored by high chain mobility and flexibility (Hoover 1995). Besides, this chain mobility is also

Table 1 Thermal parameters of the modified starches

Transition	Parameter	RS0	RS4	RSp0	RSp4
Melting of retrograded amylopectin	T_{oR} (°C)	43.9 ± 1.6c	42.3 ± 0.8bc	39.6 ± 0.8b	36.0 ± 1.5a
	T_{pR} (°C)	50.3 ± 1.5	51.2 ± 0.6	56.2 ± 1.9	52.3 ± 2.6
	T_{fR} (°C)	58.2 ± 3.4a	66.3 ± 1.6b	86.6 ± 2.5c	83.8 ± 1.9c
	ΔT_R (°C)	14.3 ± 3.8a	24.0 ± 1.8b	47.0 ± 2.6c	47.8 ± 2.4c
	ΔH_R (J/g)	0.4 ± 0.1a	1.0 ± 0.0a	7.0 ± 0.3b	8.9 ± 1.2c
Amylose–lipid complex dissociation	T_{oA-L} (°C)	89.4 ± 0.1a	89.1 ± 0.4a	94.2 ± 0.1c	92.2 ± 0.2b
	T_{pA-L} (°C)	98.6 ± 0.0a	100.2 ± 0.8b	101.8 ± 0.2c	99.8 ± 0.1b
	T_{fA-L} (°C)	108.5 ± 0.4	112.7 ± 2.0	111.2 ± 1.0	110.3 ± 0.2
	ΔT_{A-L} (°C)	19.1 ± 0.4a	23.6 ± 0.4b	17.0 ± 1.0a	18.1 ± 0.3a
	ΔH_{A-L} (J/g)	1.15 ± 0.20b	1.45 ± 0.04c	0.82 ± 0.02a	0.88 ± 0.01ab

Mean ± standard deviation. T_o, T_p, and T_f, are the onset, peak, and final temperatures, respectively. ΔT and ΔH are the temperature range and the enthalpy of the respective endotherms. The subscripts R and A-L correspond to the melting of retrograded amylopectin transition and to the amylose–lipid complex dissociation transition, respectively. Different letters in the same row indicate significant differences ($p < 0.05$; $n = 2$)

enhanced by higher temperatures (Silverio et al. 2000). In this work, the effect of the storing temperature on the transition temperatures was not completely clear probably due to the proximity of the evaluated temperatures (0 and 4 °C). However, the samples stored at 4 °C tended to higher retrogradation enthalpies than those stored at 0 °C, showing that the higher mobility favors the retrogradation.

The retrogradation process is influenced by chain length and, for amylopectin, is also linked to the ability of glucose chains to form double helices (Vamadevan and Bertoft 2014). According to the structural model of Bertoft (2013), the highly branched regions in the amylopectin molecule are composed of ca. 2–11 chains. These chains are linked along the longer glucose chains (polymerization degree higher than 35) forming blocks and constituting the structural backbone of the amylopectin molecule. Vamadevan and Bertoft (2018) studied starches of different botanical origins and found a high and positive correlation between the external chain length and different thermal parameters associated with the retrograded amylopectin melting endotherm (i.e., peak temperature, final temperature, range, and retrogradation enthalpy).

In a similar way, the debranched samples exhibited amylose–lipid complex melting transitions at higher temperatures. The T_{oA-L} of RSp0 and RSp4 were higher than that of RS0 and RS4. However, there were no differences among the T_{fA-L} of the mentioned samples. This situation led to a slightly narrower temperature range for RSp0 and RSp4 compared with RS0 and RS4 (ΔT_{A-L} in Table 1) and suggests the formation of more stable complexes but with a more cooperative melting process. Besides, a significant decrease of ΔH_{A-L} was recorded for the pullulanase-treated samples. Some authors stated that pullulanase action on amylopectin produces more linear chains, favoring the complex formation and giving higher associated enthalpies (Wongprayoon et al. 2018). However, the authors also established that retrogradation and complex formation were competitive processes when a high number of linear chains were formed. Additionally, Gelders et al. (2005) studied the formation of different amylose–lipid complex types using starches

prepared by controlled hydrolysis for obtaining polysaccharide chains with different polymerization degrees. Their results indicated that the complex formation required chains with a polymerization degree higher than 60. In the present work, the reduction of ΔH_{A-L} and the increase in ΔH_R in the pullulanase-treated samples suggest that the linear chains tended to retrogradation instead of complex formation, favored by the presence of a high number of linear chains and/or their short length.

Pasting Properties

In general, it was found that NS exhibited high viscosity under the assay conditions (Fig. 2). In fact, its pasting profile revealed high peak viscosity (η_p), followed by a marked breakdown and a subsequent increase in viscosity while cooling (setback) (Table 2). This behavior was related to the granular structure of NS, which swells and gelatinizes (amylose and amylopectin lixiviation) gaining viscosity, but then, it loses integrity due to stirring and viscosity decreases. Finally, with cooling, polymers reassociate producing an additional increase in viscosity.

In the case of RS, a marked decrease of viscosity was observed with respect to NS (Fig. 2). All retrograded starches exhibited very low or even no viscosity in suspension (values of η_p, η_{min}, and η_f in Table 2). In the case of the RS obtained only by thermal treatments (RS0 and RS4), the pasting profiles were less defined. The decrease in viscosity would be mainly associated with the absence of granular structure. However, in these samples, the setback was evident, showing the capacity of the polymers for re-association.

On the contrary, in the pullulanase-treated samples, the profiles were almost completely flat, which prevented the quantification of most of the pasting parameters. The absence of granular structure, in addition to the hydrolysis treatment in these samples, would make them unable to produce a viscous suspension, even though the smaller polysaccharide fragments could interact with each other. A similar behavior was found for retrograded sweet potato starches by Surendra Babu and Parimalavalli (2018). The authors found that the autoclaving

Fig. 2 Pasting profiles of NS and resistant starches. The orange curve represents the temperature profile (right Y-axis)
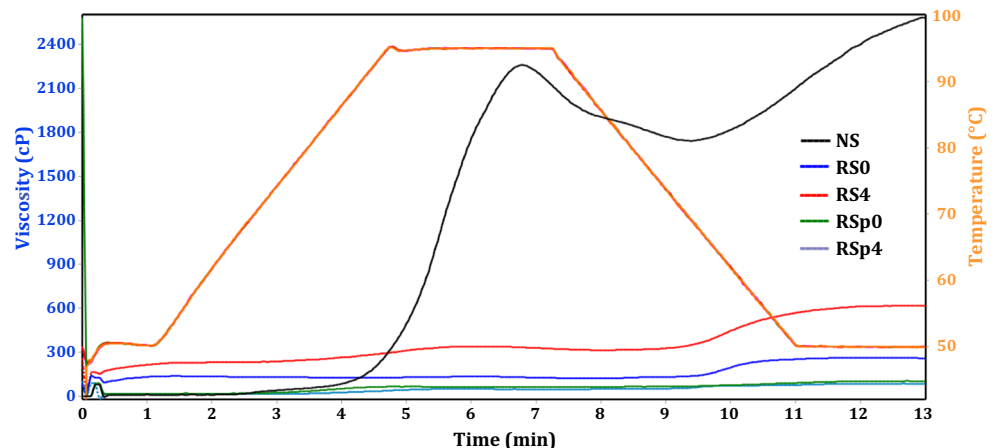
Table 2 Pasting parameters of NS and RS

Sample	NS	RS0	RS4	RSp0	RSp4
T_e (°C)	90.7 ± 0.9	nd	nd	nd	nd
t_e (min)	4.4 ± 0.1	nd	nd	nd	nd
η_p (cP)	2234 ± 38d	127 ± 11b	336 ± 8c	62 ± 4a	49 ± 1a
η_{min} (cP)	1737 ± 7c	116 ± 10a	313 ± 2b	nd	nd
η_p–η_{min} (cP)	497 ± 31b	11 ± 1a	23 ± 6a	nd	nd
η_f (cP)	2543 ± 57d	249 ± 16b	616 ± 1c	101 ± 2a	85 ± 2a
η_f–η_{min} (cP)	806 ± 50c	133 ± 6a	304 ± 1b	nd	nd
η_f–η_p (cP)	309 ± 19d	122 ± 5b	281 ± 6c	39 ± 2a	36 ± 1a

Mean ± standard deviation. T_e and t_e are the pasting temperatures and times, respectively. η_p, η_{min}, and η_f are the peak, minimum and final viscosities, respectively. Different letters in the same row indicate significant differences ($p < 0.05$; $n = 2$)

nd not detected

and pullulanase debranching treatments applied over the starch would produce a disruption of the granules, thus producing a drastic loss to the thickening capacity of the material. Moreover, Gelencsér et al. (2008) studied the pasting properties of different resistant starches (maize, tapioca, wheat), finding that all the evaluated resistant starch types presented virtually flat pasting profiles with negligible viscosity. A similar effect on pasting profiles was observed by Pratiwi et al. (2015) with suspensions of lintnerized starch (starch hydrolyzed with acid) and lintnerized-autoclaved starch.

In relation to the storage temperature, it was found that pullulanase-treated samples had no differences in the η_p, η_f, and (η_f–η_p) when stored at 0 or 4 °C. However, those samples obtained without debranching treatment showed a different behavior depending on the storage temperature. The sample stored at 0 °C (RSp0) showed less capacity to raise the viscosity of the suspension than that stored at 4 °C (RSp4), as can be seen in the corresponding pasting parameters (Table 2). The different pasting behaviors between RSp0 and RSp4 would probably be explained by differences in the establishment of interactions during retrogradation in the preparation stage.

Microstructure by LVSEM

Microscopic images of the prepared resistant starches are shown in Fig. 3. All images were characterized by the presence of starch fragments without any traces of granular structures, which indicated that NS was completely gelatinized with the applied treatments.

In the case of the RS prepared without debranching, a different morphology was found depending on the storage temperature. RS0 (Fig. 3a) mainly shows structures that could be described as densely packed fragments with irregular polygonal shapes (filled arrows), with little presence of other particles of irregular porous appearance (hyphenated arrows). On the

contrary, RS4 (Fig. 3b) exhibited mainly porous and irregularly shaped structures (hyphenated arrows), with the random presence of more compact fragments that show smooth surfaces (filled arrows). These differences in morphology could explain the pasting properties of these starches, since they exhibited different thickening capacity. The greater presence of porous structures in RS4 would be responsible for the higher viscosity exhibited by this sample likely due to a higher hydration capacity of this kind of structure. On the contrary, the compact structures in RS0 would find difficulties for proper hydration, leading to a lower thickening capacity.

In general, the starches treated with pullulanase showed similar microstructure. In this case, two kinds of dense structures were identified in both RSp0 (Fig. 3c) and RSp4 (Fig. 3d): fragments with regular fine-textured surfaces and sharp edges (filled arrows) and fragments with irregular coarse surfaces (hyphenated arrows). The latter seem to be composed of overlapped layers. The high presence of these compact structures would explain the low thickening capacity of these samples, since these highly packed fragments would be less hydratable. Moreover, the similarity found between RSp0 and RSp4 in the micrographs would be in accord with the similar pasting behavior exhibited by these samples.

The structures observed in the present work are in accordance with several authors. Surendra Babu and Parimalavalli (2018) described similar structures when observing retrograded sweet potato starches, prepared by autoclaving and debranching, by SEM, and the same was also made by Van Hung et al. (2012) with cassava and potato starches, and Polesi and Sarmento (2011) with chickpea starch. Moreover, Okumus et al. (2018) showed that these structures were also present in retrograded lentil starch prepared by cooking and subsequent lipid complexation to form type V resistant starch, and this was also seen by Wongprayoon et al. (2018) on cassava, rice, and chickpea starches that were debranched previous to the lipid complexation.

Crystallinity

The NS (Fig. 4(a)) exhibited a typical pattern for native cereal starches, characterized by an A-type crystalline arrangement with an intense doublet at 17° 2θ, two intense peaks at 15 and 23°, and a lower peak at 20°. This last peak was commonly associated with a V-type pattern, related to the presence of the amylose–lipid complex (Román et al. 2016). On the other hand, Fig. 4(b) shows the diffraction pattern of the gelatinized wheat starch. In this sample, the peak at 20° 2θ suggests the presence of the amylose–lipid complex. However, the absence of other intense peaks indicates that this sample was composed mainly of amorphous phase.

Patterns c and d in Fig. 4 show the spectra obtained for RS0 and RS4, respectively. These samples exhibited wide Gaussian-type patterns that indicate major predominance of
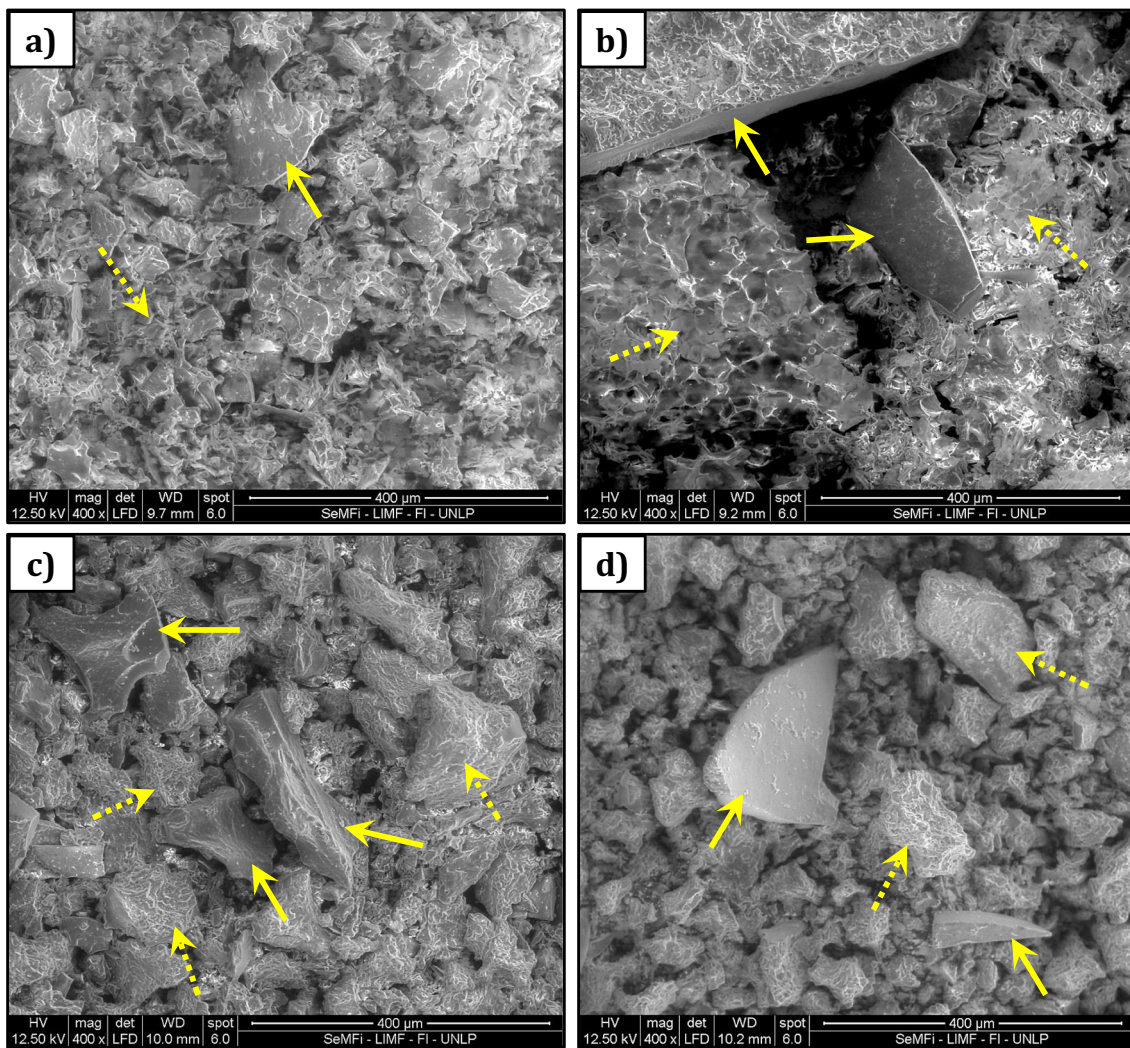
Fig. 3 Microscopy images of RS at 400 ×. **a** RS0 and **b** RS4, where filled arrows point to compact structures and hyphenated arrows to irregular and porous structures. **c** RSp0 and **d** RSp4, where filled arrows point to flat and sharpened structures and hyphenated arrows to irregular structures

amorphous phase. However, low-intensity single peaks could be detected at 17, 20, and 23° 2θ, indicating that these samples gained certain B-type crystallinity from retrogradation.

In the case of RSp0 (Fig. 4(e)) and RSp4 (Fig. 4(f)), the effect was more noticeable. Both samples exhibited single strong diffraction peaks at 17° 2θ and other smaller peaks at 15, 20, and 23°, giving a B-type crystalline structure. The more defined patterns shown by RSp0 and RSp4 indicate that a more crystalline retrograded starch was obtained with pullulanase treatment.

Due to the polymorphism occurring while processing starch, several authors have studied the enzymatic susceptibility of A- and B-type polymorphs isolated from different starch sources by lintnerization, further modification, and purification. Then, the authors found that B-type allomorphs were more stable to hydrolysis than the A-type (Planchot et al. 1997; Williamson et al. 1992). However, in recent studies, Cai and Shi (2014) concluded that the type of crystalline

arrangement was not the main factor for predicting enzymatic susceptibility, and also that obtaining high crystallinity yields would not guarantee higher enzymatic resistance by the product. Instead, the resistance to enzymatic digestion would be determined by the perfection of the crystallites, no matter the type of polymorph present. Then, they indicated that starch modification processes focused on efficient packaging of the polysaccharides during storage would enhance the enzymatic resistance of retrograded starches.

Starch Digestibility and Estimated GI

The evaluation of the enzymatic susceptibility of the modified starches was assessed in vitro using α-amylase (Fig. 5). The curve for cooked NS showed pronounced hydrolysis extension and high hydrolysis rate, with the highest values of C_∞ and k (Table 3). However, thermal and enzymatic-thermal modifications of the NS produced retrograded starches with

Fig. 4 X-ray diffraction patterns: (a) NS, (b) gelatinized starch, (c) RS0, (d) RS4, (e) RSp0, and (f) RSp4
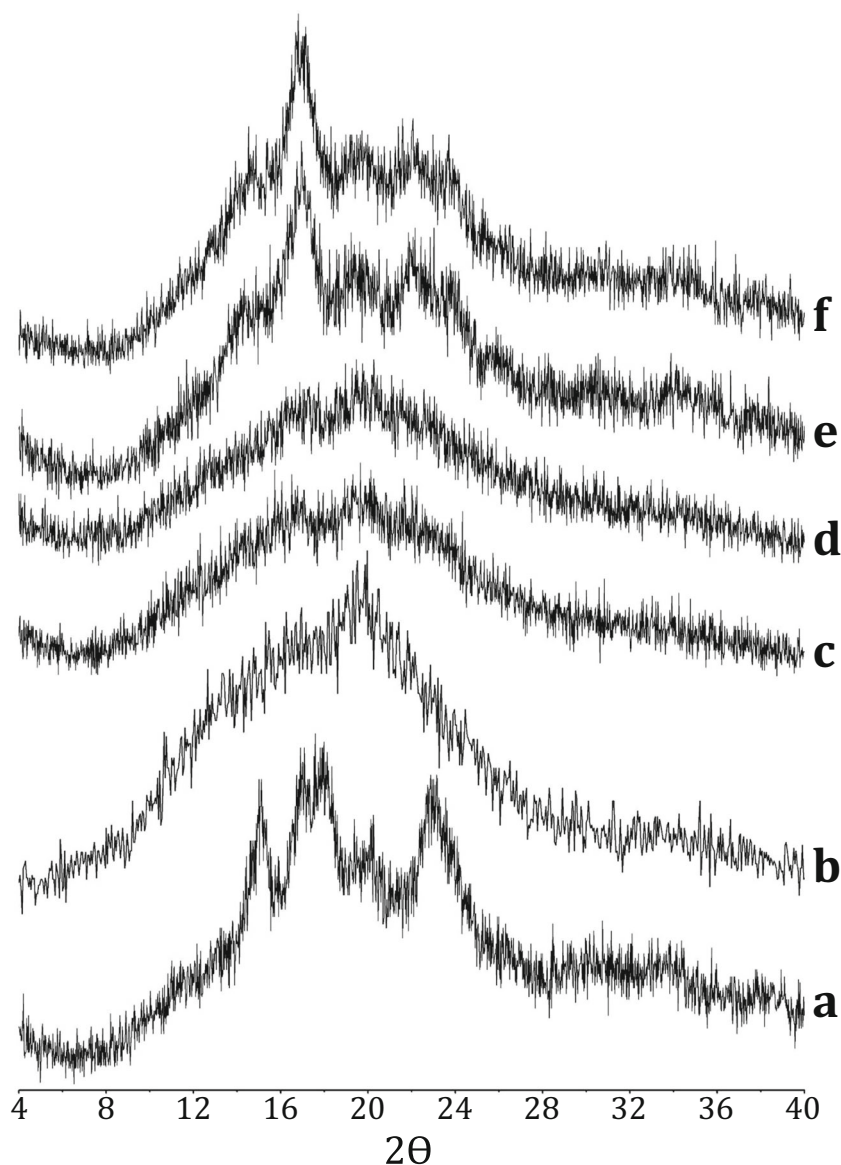
less limit digestibility and slower hydrolysis rates, both effects related to healthier products (Montonen et al. 2003; Willett et al. 2002). This effect was more pronounced in the sample stored at 0 °C (RS0) and even more marked in both pullulanase-treated samples (Table 3).

The differences between RS0 and RS4 were associated with their microstructure, since RS0 was composed of compact starch fragments and RS4 presented porous and open structures in its composition. As also seen in the RVA assays, the more porous structure in RS4 led to a higher thickening capacity and would indicate a better unfolding of the starch polymers, the latter being more accessible to α-amylase action. These results are in accordance with those reported by Hódsági et al. (2012). In their work, the authors found strong and positive correlations among the RVA parameters and the

digestibility characteristics of mixtures of native starches with type II or type III resistant starches, showing that low viscosity values in the RVA method positively correlated with lower releases of reducing sugars by enzymatic hydrolysis.

In the case of RSp0 and RSp4, the decreased and slower digestibility was associated with the high presence of compact structures in their composition and the consequent absence of thickening capacity, as discussed above. Also, these samples were considered to achieve more retrograded material, as seen in their melting enthalpies in DSC assays and in their narrower patterns in the X-ray diffraction experiments. In this aspect, Liu et al. (2017) stated that the linear chains released by hydrolysis can better align each other and re-associate. Then, the aggregation of such structures forms crystals that are refractory to the enzymes action, and thus debranched starch can be a
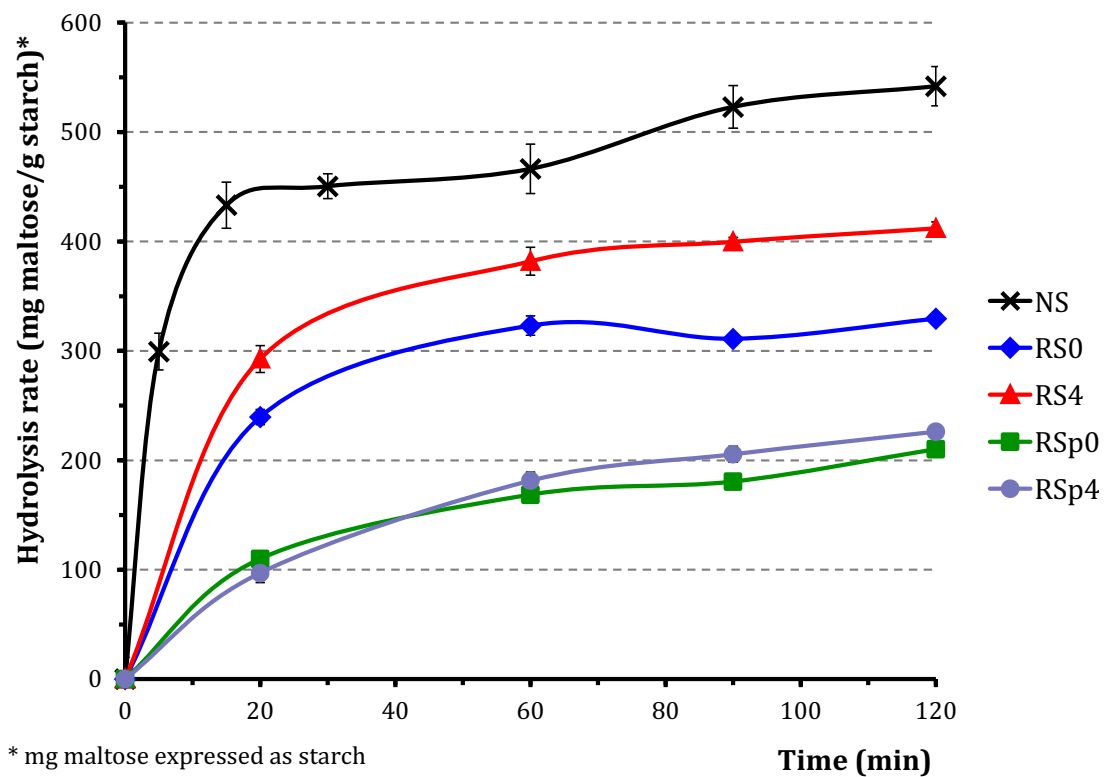
Fig. 5 Hydrolysis rate mean curves of native and modified starches

good source of resistant starch. The authors also claimed that not only high-amylose starches, but also native starches containing amylose, are better for producing resistant starch, while waxy starches are more prone to yield slowly digestible starch.

These results indicate that the application of the proposed treatments to native wheat starch would reduce the impact of this starch on glycemia after its consumption. The estimated values for the GI are shown in Table 3. In the case of the

thermally treated starches, the reduction of the estimated GI was ca. 25% (RS4) and 39% (RS0), while for the enzymatic thermally treated samples, the reduction was as great as ca. 66% for both RSp0 and RSp4 samples. Wandee et al. (2012) reported that a more destructive heat treatment over canna starch samples yielded more resistant starch and slowly digestible starch than when the same starches were subjected to a less aggressive heating. This phenomenon was attributed to a higher level of granule disintegration that led to a greater possibility of effective association of amylopectin chains. Then, the authors concluded that the yield of resistant canna starch would be enhanced by using enzymes such as amylase and pullulanase. In the same way, Khan et al. (2019) reported that resistant starch prepared by hydrolysis of maize starch was less digestible than the native one when going through a gastrointestinal simulation protocol. Besides, the treatments applied to the starch also rendered a compact crystalline structure as described in LVSEM. In the present work, the retrogradation enthalpy of stored wheat starch pastes was indeed markedly increased when pullulanase was employed, indicating greater association of amylopectin chains. This also led to a reduced viscosity, digestibility, and estimated GI and would confirm that a higher disintegration of the granular structure of the wheat starch previous to the storage would be a suitable choice for obtaining type III resistant starch. Such decrease in the potential glycemic response of all the obtained starches,

Table 3 Kinetic parameters of the hydrolysis with α-amylase of NS and the obtained RS

	C_∞ (mg/g)*	k (min^{-1})	Adj. r^2	F test	Est. GI
NS[†]	489 ± 10	0.168 ± 0.021	0.9256	a	100
RS0	323 ± 4	0.068 ± 0.005	0.9890	b	61.0
RS4	402 ± 5	0.064 ± 0.004	0.9918	c	75.2
RSp0	199 ± 6	0.036 ± 0.004	0.9646	d	33.1
RSp4	233 ± 6	0.026 ± 0.002	0.9882	e	34.6

Value ± standard error. C_∞ and k are the limit digestibility and the constant rate, respectively. *Est. GI* is the estimated glycemic index. Different letters in the F tests indicate significant differences between datasets ($p < 0.05$; $n = 2$)

*Expressed as mg maltose/g starch, maltose expressed as starch

[†] NS = native wheat starch

but especially the pullulanase-treated ones, would exert benefits over consumer's health in comparison with traditional non-modified starches.

Conclusions

Type III resistant starches were obtained by thermal and enzymatic-thermal modifications of native wheat starch. The retrogradation temperature showed no influence on the pullulanase-treated starches but affected the microstructure of those obtained only by the thermal treatment, then allowing the production of two products differing in their pasting properties and digestibility. In this case, a storing temperature of 0 °C would be advantageous since a more compact and less digestible product was obtained. In a similar way, the storage of the pullulanase-treated samples at 4 °C would be convenient from an economic point of view since no differences were found between RSp0 and RSp4.

Finally, even though all the obtained products exhibited a significant reduction in their digestibility, the combination of the pullulanase-debranching step with 4 cycles of heating and cooling was more effective in yielding a greater retrograded phase, as found in DSC and X-ray experiments. Moreover, these products were markedly more resistant to enzymatic α-amylase digestion and led to a reduction of 66% in the in vitro estimated glycemic index with respect to the native wheat starch. The low digestibility was attributed to the high retrogradation extension and the compact microstructure that these starches exhibited. These results confirm that wheat starch could be a good source of type III resistant starch. The application of the adequate methods allows obtaining a healthy ingredient that could be incorporated as fiber into different foods, such as dairy products, cereal bars, and drinks, probably without substantially changing the organoleptic profile due to their characteristics and low thickening capacity.

and Consejo Nacional de Investigaciones Científicas y Técnicas (CONICET).

References

AACC International. (2009). Method 76-21.01 - general pasting method for wheat or rye flour of starch using the rapid visco analyser. In *AACC international approved methods* (pp. 7–10). AACC International. https://doi.org/10.1094/AACCIntMethod-76-21.01.

Arp, C. G., Correa, M. J., & Ferrero, C. (2018). High-amylose resistant starch as a functional ingredient in breads: a technological and microstructural approach. *Food and Bioprocess Technology, 11*(12), 2182–2193. https://doi.org/10.1007/s11947-018-2168-4.

Ashwar, B. A., Gani, A., Shah, A., Wani, I. A., & Masoodi, F. A. (2016). Preparation, health benefits and applications of resistant starch - a review. *Starch/Staerke, 68*(3–4), 287–301. https://doi.org/10.1002/star.201500064.

Bello-Perez, L. A., & Hoyos-Leyva, J. D. (2018). Development of foods high in slowly digestible and resistant starch. In M. Sjöö & L. Nilsson (Eds.), *Starch in food* (2nd ed., pp. 827–854). Cambridge: Elsevier. https://doi.org/10.1016/B978-0-08-100868-3.00022-6.

Bertoft, E. (2013). On the building block and backbone concepts of amylopectin structure. *Cereal Chemistry, 90*(4), 294–311. https://doi.org/10.1094/CCHEM-01-13-0004-FI.

Brumovsky, L. A., Brumovsky, J. O., Fretes, M. R., & Peralta, J. M. (2009). Quantification of resistant starch in several starch sources treated thermally. *International Journal of Food Properties, 12*(3), 451–460. https://doi.org/10.1080/10942910701867673.

Cai, L., & Shi, Y. C. (2014). Preparation, structure, and digestibility of crystalline A- and B-type aggregates from debranched waxy starches. *Carbohydrate Polymers, 105*(1), 341–350. https://doi.org/10.1016/j.carbpol.2014.01.075.

Champ, M. (2004). Resistant starch. In A.-C. Eliasson (Ed.), *Starch in food* (Vol. 38, 1st ed., pp. 560–574). Cambridge: Woodhead Publishing Limited. https://doi.org/10.1533/9781855739093.4.560.

Chang, R., Tian, Y., Lu, H., Sun, C., & Jin, Z. (2020). Effects of fractionation and heat-moisture treatment on structural changes and digestibility of debranched waxy maize starch. *Food Hydrocolloids, 101*(October 2019), 105488. https://doi.org/10.1016/j.foodhyd.2019.105488.

Chávez-Murillo, C. E., Veyna-Torres, J. I., Cavazos-Tamez, L. M., de la Rosa-Millán, J., & Serna-Saldívar, S. O. (2018). Physicochemical characteristics, ATR-FTIR molecular interactions and in vitro starch and protein digestion of thermally-treated whole pulse flours. *Food Research International, 105*(December 2016), 371–383. https://doi.org/10.1016/j.foodres.2017.11.029.

Cordoba, L. d. P., da Silva, R. G., Gomes, D. d. S., Schnitzler, E., & Waszczynskyj, N. (2018). Brazilian green banana - a thermal, structural and rheological investigation of resistant starch from different cultivars. *Journal of Thermal Analysis and Calorimetry, 134*(3), 2065–2073. https://doi.org/10.1007/s10973-018-7374-9.

Dong, H., & Vasanthan, T. (2020). Amylase resistance of corn, faba bean, and field pea starches as influenced by three different phosphorylation (cross-linking) techniques. *Food Hydrocolloids, 101*(November 2019), 105506. https://doi.org/10.1016/j.foodhyd.2019.105506.

Dundar, A. N., & Gocmen, D. (2013). Effects of autoclaving temperature and storing time on resistant starch formation and its functional and

physicochemical properties. *Carbohydrate Polymers, 97*(2), 764–771. https://doi.org/10.1016/j.carbpol.2013.04.083.

Gelders, G. G., Duyck, J. P., Goesaert, H., & Delcour, J. A. (2005). Enzyme and acid resistance of amylose-lipid complexes differing in amylose chain length, lipid and complexation temperature. *Carbohydrate Polymers, 60*(3), 379–389. https://doi.org/10.1016/j.carbpol.2005.02.008.

Gelencsér, T., Juhász, R., Hódsági, M., Gergely, S., & Salgó, A. (2008). Comparative study of native and resistant starches. *Acta Alimentaria, 37*(2), 255–270. https://doi.org/10.1556/AAlim.37.2008.2.11.

Goñi, I., Garcia-Alonso, A., & Saura-Calixto, F. (1997). A starch hydrolysis procedure to estimate glycemic index. *Nutrition Research, 17*(3), 427–437. https://doi.org/10.1016/S0271-5317(97)00010-9.

Gopalsamy, G., Mortimer, E., Greenfield, P., Bird, A. R., Young, G. P., & Christophersen, C. T. (2019). Resistant starch is actively fermented by infant faecal microbiota and increases microbial diversity. *Nutrients, 11*(6), 1345. https://doi.org/10.3390/nu11061345.

Hódsági, M., Gelencsér, T., Gergely, S., & Salgó, A. (2012). In vitro digestibility of native and resistant starches: correlation to the change of its rheological properties. *Food and Bioprocess Technology, 5*(3), 1038–1048. https://doi.org/10.1007/s11947-010-0391-8.

Hoover, R. (1995). Starch retrogradation. *Food Reviews International, 11*(2), 331–346. https://doi.org/10.1080/87559129509541044.

Jiang, F., Du, C., Jiang, W., Wang, L., & Du, S. (2020). The preparation, formation, fermentability, and applications of resistant starch. *International Journal of Biological Macromolecules, 150*, 1155–1161. https://doi.org/10.1016/j.ijbiomac.2019.10.124.

Khan, A., Rahman, U. U., Siddiqui, S., Irfan, M., Shah, A. A., Badshah, M., Hasan, F., & Khan, S. (2019). Preparation and characterization of resistant starch type III from enzymatically hydrolyzed maize flour. *Molecular Biology Reports, 46*(4), 4565–4580. https://doi.org/10.1007/s11033-019-04913-5.

Kovrlija, R., & Rondeau-Mouro, C. (2017). Hydrothermal changes of starch monitored by combined NMR and DSC methods. *Food and Bioprocess Technology, 10*(3), 445–461. https://doi.org/10.1007/s11947-016-1832-9.

Li, T., Chen, L., Xiao, J., An, F., Wan, C., & Song, H. (2018). Prebiotic effects of resistant starch from purple yam (Dioscorea alata L.) on the tolerance and proliferation ability of Bifidobacterium adolescentis in vitro. *Food & Function, 9*(4), 2416–2425. https://doi.org/10.1039/C7FO01919J.

Liu, H., Liang, R., Antoniou, J., Liu, F., Shoemaker, C. F., Li, Y., & Zhong, F. (2014). The effect of high moisture heat-acid treatment on the structure and digestion property of normal maize starch. *Food Chemistry, 159*, 222–229. https://doi.org/10.1016/j.foodchem.2014.02.162.

Liu, G., Gu, Z., Hong, Y., Cheng, L., & Li, C. (2017). Structure, functionality and applications of debranched starch: a review. *Trends in Food Science & Technology, 63*, 70–79. https://doi.org/10.1016/j.tifs.2017.03.004.

Montonen, J., Knekt, P., Järvinen, R., Aromaa, A., & Reunanen, A. (2003). Whole-grain and fiber intake and the incidence of type 2 diabetes. *The American Journal of Clinical Nutrition, 77*(3), 622–629. https://doi.org/10.1093/ajcn/77.3.622.

Okumus, B. N., Tacer-Caba, Z., Kahraman, K., & Nilufer-Erdil, D. (2018). Resistant starch type V formation in brown lentil (Lens culinaris Medikus) starch with different lipids/fatty acids. *Food Chemistry, 240*(April 2017), 550–558. https://doi.org/10.1016/j.foodchem.2017.07.157.

Öztürk, S., & Köksel, H. (2014). Production and characterisation of resistant starch and its utilisation as food ingredient: a review. *Quality Assurance & Safety of Crops and Food, 6*(3), 335–346. https://doi.org/10.3920/QAS2013.0367.

Planchot, V., Colonna, P., & Buleon, A. (1997). Enzymatic hydrolysis of α-glucan crystallites. *Carbohydrate Research, 298*(4), 319–326. https://doi.org/10.1016/S0008-6215(96)00317-5.

Polesi, L. F., & Sarmento, S. B. S. (2011). Structural and physicochemical characterization of RS prepared using hydrolysis and heat treatments of chickpea starch. *Starch - Stärke, 63*(4), 226–235. https://doi.org/10.1002/star.201000114.

Pratiwi, W. S. W., Anal, A. K., & Putra, S. R. (2015). Production by lintnerization-autoclaving and physicochemical characterization of resistant starch III from sago palm (*Metroxylon sagu* Rottb). *Indonesian Journal of Chemistry, 15*(3), 295–304. https://doi.org/10.22146/ijc.21199.

Pratiwi, M., Faridah, D. N., & Lioe, H. N. (2018). Structural changes to starch after acid hydrolysis, debranching, autoclaving-cooling cycles, and heat moisture treatment (HMT): a review. *Starch - Stärke, 70*(1–2), 1700028. https://doi.org/10.1002/star.201700028.

Remya, R., Jyothi, A. N., & Sreekumar, J. (2018). Effect of chemical modification with citric acid on the physicochemical properties and resistant starch formation in different starches. *Carbohydrate Polymers, 202*(August), 29–38. https://doi.org/10.1016/j.carbpol.2018.08.128.

Román, L., Dura, Á., Martínez, M. M., Rosell, C. M., & Gómez, M. (2016). Combination of extrusion and cyclodextrin glucanotransferase treatment to modify wheat flours functionality. *Food Chemistry, 199*, 287–295. https://doi.org/10.1016/j.foodchem.2015.12.040.

Shi, J., Sweedman, M. C., & Shi, Y.-C. (2018). Structural changes and digestibility of waxy maize starch debranched by different levels of pullulanase. *Carbohydrate Polymers, 194*(January), 350–356. https://doi.org/10.1016/j.carbpol.2018.04.053.

Silverio, J., Fredriksson, H., Andersson, R., Eliasson, A.-C., & Åman, P. (2000). The effect of temperature cycling on the amylopectin retrogradation of starches with different amylopectin unit-chain length distribution. *Carbohydrate Polymers, 42*(2), 175–184. https://doi.org/10.1016/S0144-8617(99)00140-X.

Surendra Babu, A., & Parimalavalli, R. (2018). Effect of pullulanase debranching and storage temperatures on structural characteristics and digestibility of sweet potato starch. *Journal of the Saudi Society of Agricultural Sciences, 17*(2), 208–216. https://doi.org/10.1016/j.jssas.2016.04.005.

Vamadevan, V., & Bertoft, E. (2014). Structure-function relationships of starch components. *Starch - Stärke, 66*(1-2), 1–14. https://doi.org/10.1002/star.201400188.

Vamadevan, V., & Bertoft, E. (2018). Impact of different structural types of amylopectin on retrogradation. *Food Hydrocolloids, 80*, 88–96. https://doi.org/10.1016/j.foodhyd.2018.01.029.

Van Hung, P., Lan Phi, N. T., & Vy Vy, T. T. (2012). Effect of debranching and storage condition on crystallinity and functional properties of cassava and potato starches. *Starch - Stärke, 64*(12), 964–971. https://doi.org/10.1002/star.201200039.

Van Hung, P., Binh, V. T., Nhi, P. H. Y., & Phi, N. T. L. (2020). Effect of heat-moisture treatment of unpolished red rice on its starch properties and in vitro and in vivo digestibility. *International Journal of Biological Macromolecules, 154*, 1–8. https://doi.org/10.1016/j.ijbiomac.2020.03.071.

Wandee, Y., Puttanlek, C., Rungsardthong, V., Puncha-arnon, S., & Uttapap, D. (2012). Effects of gelatinization and gel storage conditions on the formation of canna resistant starch. *Food and Bioprocess Technology, 5*(7), 2665–2673. https://doi.org/10.1007/s11947-011-0629-0.

Willett, W., Manson, J., & Liu, S. (2002). Glycemic index, glycemic load, and risk of type 2 diabetes. *The American Journal of Clinical Nutrition, 76*(1), 274S–280S. https://doi.org/10.1093/ajcn/76.1.274S.

Williamson, G., Belshaw, N. J., Self, D. J., Noel, T. R., Ring, S. G., Cairns, P., et al. (1992). Hydrolysis of A- and B-type crystalline

polymorphs of starch by α-amylase, β-amylase and glucoamylase 1. *Carbohydrate Polymers, 18*(3), 179–187. https://doi.org/10.1016/0144-8617(92)90062-U.

Wong, T. H. T., & Louie, J. C. Y. (2017). The relationship between resistant starch and glycemic control: a review on current evidence and possible mechanisms. *Starch - Stärke, 69*(7–8), 1600205. https://doi.org/10.1002/star.201600205.

Wongprayoon, S., Tran, T., Gibert, O., Dubreucq, E., Piyachomkwan, K., & Sriroth, K. (2018). Pullulanase debranching of various starches upgrades the crystalline structure and thermostability of starch-lauric acid complexes. *Starch/Staerke, 70*(7-8), 1–11. https://doi.org/10.1002/star.201700351.

Yadav, B. S., Sharma, A., & Yadav, R. B. (2010). Effect of storage on resistant starch content and in vitro starch digestibility of some pressure-cooked cereals and legumes commonly used in India. *International Journal of Food Science and Technology, 45*(12), 2449–2455. https://doi.org/10.1111/j.1365-2621.2010.02214.x.

Yu, Z., Wang, Y. S., Chen, H. H., Li, Q. Q., & Wang, Q. (2018). The gelatinization and retrogradation properties of wheat starch with the addition of stearic acid and sodium alginate. *Food Hydrocolloids, 81*, 77–86. https://doi.org/10.1016/j.foodhyd.2018.02.041.

Zhang, H., & Jin, Z. (2011). Preparation of resistant starch by hydrolysis of maize starch with pullulanase. *Carbohydrate Polymers, 83*(2), 865–867. https://doi.org/10.1016/j.carbpol.2010.08.066.

Zhao, X., Andersson, M., & Andersson, R. (2018). Resistant starch and other dietary fiber components in tubers from a high-amylose potato. *Food Chemistry, 251*(September 2017), 58–63. https://doi.org/10.1016/j.foodchem.2018.01.028.